environmental microbiology

Environmental Microbiology (2022) **24**(3), 1263–1278 doi:10.1111/1462-2920.15812

Differential response to prey quorum signals indicates predatory specialization of myxobacteria and ability to predate *Pseudomonas aeruginosa*

Shukria Akbar,[1] Kayleigh E. Phillips,[1] Sandeep K. Misra,[1] Joshua S. Sharp[1,2] and D. Cole Stevens[1*]

[1]*Department of BioMolecular Sciences, University of Mississippi, University, MS.*

[2]*Department of Chemistry and Biochemistry, University of Mississippi, University, University, MS.*

Summary

Multiomic analysis of transcriptional and metabolic responses from the predatory myxobacteria *Myxococcus xanthus* and *Cystobacter ferrugineus* exposed to prey signalling molecules of the acylhomoserine lactone and quinolone quorum signalling classes provided insight into predatory specialization. Acylhomoserine lactone quorum signals elicited a general response from both myxobacteria. We suggest that this is likely due to the generalist predator lifestyles of myxobacteria and ubiquity of acylhomoserine lactone signals. We also provide data that indicates the core homoserine lactone moiety included in all acylhomoserine lactone scaffolds to be sufficient to induce this general response. Comparing both myxobacteria, unique transcriptional and metabolic responses were observed from *Cystobacter ferrugineus* exposed to the quinolone signal 2-heptylquinolin-4(1*H*)-one (HHQ) natively produced by *Pseudomonas aeruginosa*. We suggest that this unique response and ability to metabolize quinolone signals contribute to the superior predation of *P. aeruginosa* observed from *C. ferrugineus*. These results further demonstrate myxobacterial eavesdropping on prey signalling molecules and provide insight into how responses to exogenous signals might correlate with prey range of myxobacteria.

Received 11 June, 2021; revised 20 September, 2021; accepted 7 October, 2021. *For correspondence. Tel: 662-915-5730; Fax: 662-915-5638; E-mail stevens@olemiss.edu

Introduction

The uniquely multicellular lifestyles of myxobacteria have motivated continued efforts to explore the myxobacterium *Myxococcus xanthus* as a model organism for cooperative behaviours including development (Islam *et al*., 2020; Sharma *et al*., 2021), motility (Mercier *et al*., 2020; Rendueles and Velicer, 2020; Zhang *et al*., 2020b), and predation (Thiery and Kaimer, 2020; Zhang *et al*., 2020a; Sydney *et al*., 2021). Often attributed to their need to acquire nutrients as generalist predators (Nair *et al*., 2019) and capacity to prey upon clinical pathogens (Livingstone *et al*., 2017), myxobacteria have also been a valuable resource for the discovery of novel specialized metabolites as potential therapeutic lead compounds (Herrmann *et al*., 2017; Baltz, 2019; Perez *et al*., 2020). The diversities in structural scaffolds and observed activities as well as the unique chemical space associated with myxobacterial metabolites when compared with more thoroughly explored Actinobacteria make myxobacteria excellent sources for efforts focused on the discovery of therapeutics (Herrmann *et al*., 2017; Baltz, 2019). However, the connection between myxobacterial predation and production of these biologically active metabolites remains underexplored. Currently, only the metabolites myxovirescin (Xiao *et al*., 2011; Ellis *et al*., 2019; Wang *et al*., 2019) and myxoprincomide (Cortina *et al*., 2012; Muller *et al*., 2016) have been directly implicated to be involved during *Myxococcus xanthus* predation of *Escherichia coli* and *Bacillus subtilis*, respectively. In fact, the chemical ecology of predator–prey interactions between myxobacteria and prey remains underexplored (Findlay, 2016). The predatory capacity or prey range of myxobacteria cannot be directly correlated with phylogeny (Livingstone *et al*., 2017; Arend *et al*., 2020). Presently, the best determinants for broadly assessing prey ranges are genetic features that might provide specific traits to overcome predation resistances of individual prey. For example, myxobacteria possessing the formaldehyde dismutase gene *fdm* demonstrated comparatively better predation of toxic formaldehyde secreting *Pseudomonas aeruginosa* an opportunistic pathogen observed to be somewhat

© 2021 The Authors. *Environmental Microbiology* published by Society for Applied Microbiology and John Wiley & Sons Ltd. This is an open access article under the terms of the Creative Commons Attribution License, which permits use, distribution and reproduction in any medium, provided the original work is properly cited.

recalcitrant to myxobacterial predation (Sutton *et al*., 2019).

The recent observation that acylhomoserine lactone (AHL) quorum signals from prey microbes impact the predatory capacity of *M. xanthus* suggests that quorum signals might influence predator–prey interactions (Lloyd and Whitworth, 2017). Although two orphaned, functional AHL synthases have been reported, no myxobacteria have been observed to produce AHLs (Albataineh *et al*., 2021). However, a recent survey of signalling systems within the family Myxococcaceae reported the presence of conserved AHL receptor (LuxR) homologues and inferred that many myxobacteria within the two genera *Myxococcus* and *Corallococcus* are capable of sensing AHL signalling molecules (Whitworth and Zwarycz, 2020). While this suggests that predatory myxobacteria might eavesdrop on prey quorum signalling, the observed reaction from *M. xanthus* might also simply be the result of exogenous AHLs as a nutrient source. Herein we utilize a combination of transcriptomics and metabolomics to determine how myxobacterial responses to quorum signals produced by *P. aeruginosa* might indicate predatory capacity.

By exposing myxobacteria to structurally and functionally distinct classes of prey quorum signals comparing ubiquitous AHL signals and quinolone signals more unique to pseudomonads (Papenfort and Bassler, 2016), we anticipated that a differential response exclusive to a specific signal class would support predatory eavesdropping and perhaps correlate with improved predation of *P. aeruginosa*. For these experiments we exposed each myxobacterium to AHL signals (Galloway *et al*., 2011) as well as the quinolone signal 2-heptylquinolin-4(1*H*)-one (HHQ; Deziel *et al*., 2004; Dubern and Diggle, 2008; Garcia-Reyes *et al*., 2020). Ubiquitous to Proteobacteria (notably excluding myxobacteria) and numerous other non-Proteobacteria genera, AHLs are the most common class of quorum signal autoinducers and are often implicated in interspecies communication within polymicrobial communities (Shiner *et al*., 2005; Mukherjee and Bassler, 2019). Also associated with the modulation of interspecies and interkingdom behaviours (Reen *et al*., 2011), the quinolone signal HHQ contributes to the pathogenicity of *P. aeruginosa* by participating in the regulation of various virulence factors (Dubern and Diggle, 2008; Reen *et al*., 2011). Exploration of the myxobacterial response to prey quorum signals not only provides insight into the impact of shared chemical signals might have on predator–prey interactions within bacterial communities but may also provide further genetic determinants that indicate predatory capacities of myxobacteria.

As a model organism for developmental studies, *M. xanthus* is the best characterized myxobacterium and has already demonstrated a behavioural response to exogenous AHLs (Lloyd and Whitworth, 2017). However, we suspected that routine use as a laboratory strain and well-explored specialized metabolism (Cortina *et al*., 2012; Herrmann *et al*., 2017) of *M. xanthus* might diminish its viability as the sole myxobacterium for these experiments. Also of note, *M. xanthus* constitutively secretes lytic enzymes and specialized metabolites associated with prey lysis which may limit observable transcriptomic and metabolomic responses to exogenous quorum signals (Livingstone *et al*., 2018). Therefore, *Cystobacter ferrugineus* was also included as a more recent myxobacterial isolate with a less explored biosynthetic capacity and prey range (Akbar *et al*., 2017; Goes *et al*., 2020). Both *M. xanthus* and *C. ferrugineus* have an annotated solo LuxR-type AHL receptor present in their genomes (WP_011555271.1 and WP_071900454.1; Subramoni and Venturi, 2009; Tobias *et al*., 2020; Xu, 2020). However, homology-based annotation of these features only indicates the helix–turn–helix DNA-binding domain of LuxR receptors, and neither include an AHL-binding site motif (PF03472; Baikalov *et al*., 1996; Vannini *et al*., 2002; Mukherjee and Bassler, 2019). Despite the absence of a canonical receptor, exogenous AHLs have been observed to stimulate the motility and predatory activity of *M. xanthus* (Lloyd and Whitworth, 2017). Also of note, neither *M. xanthus* or *C. ferrugineus* possess a homologous PqsR-type HHQ receptor (Diggle *et al*., 2003; Wade *et al*., 2005). Utilizing a multiomic approach to assess the transcriptomic and metabolomic responses of *M. xanthus* and *C. ferrugineus* when exposed to AHL and quinolone signals, we sought to determine if structurally and functionally dissimilar quorum signals from prey elicit distinct responses from predatory myxobacteria that correlate with successful predation of *P. aeruginosa*.

Results

C6-AHL induces a general transcriptional response from both M. xanthus *and* C. ferrugineus

Exposure experiments utilizing a concentration of C6-AHL previously shown to elicit a predatory response from *M. xanthus* (9 μM) were conducted on plates of *M. xanthus* and *C. ferrugineus* (Lloyd and Whitworth, 2017). Exposure experiments were conducted in triplicate for both *M. xanthus* and *C. ferrugineus* with DMSO exposures serving as vehicle, negative controls for comparative analysis. Comparative transcriptomic analysis from RNAseq data revealed C6-AHL exposure impacted transcription of a total of 76 genes from *C. ferrugineus* experiments and just nine genes from *M. xanthus* experiments when only considering a ≥4-fold

© 2021 The Authors. *Environmental Microbiology* published by Society for Applied Microbiology and John Wiley & Sons Ltd.,

change in transcription at $p \leq 0.01$ (Fig. 1, Appendix S1). For this reason, our analysis of *M. xanthus* exposure experiments was expanded to include significant features at $p \leq 0.05$ resulting in an updated total of 56 impacted features from C6-AHL exposure (Fig. 1). While this indicates less variability across *C. ferrugineus* exposure experiments, we contend that this expansion provides a broader and more thorough analysis of statistically significant impacted features for our analysis. A similar consideration of *C. ferrugineus* genes with ≥4-fold change in transcription at $p \leq 0.05$ by C6-AHL exposure would provide an additional 119 impacted genes for consideration (Appendix S1). *M. xanthus* features included at the more stringent significance cutoff of $p \leq 0.01$ are indicated in Fig. 1. These data revealed that C6-AHL exposure elicited a general downregulation of genes with a total of 55 downregulated genes observed from *M. xanthus* and 51 genes from *C. ferrugineus*. Only one gene was observed to be upregulated by *M. xanthus* when exposed to C6-AHL, and 25 total upregulated genes were observed from *C. ferrugineus* during C6-AHL exposure.

Comparing annotated features impacted by C6-AHL exposure across both datasets and their putative roles by general system, numerous features involved in signal transduction pathways and transcriptional regulation were included in both datasets with seven regulatory features downregulated by *M. xanthus* and six downregulated by *C. ferrugineus* (Fig. 2). Both myxobacteria also had a TetR family transcriptional regulator upregulated by C6-AHL exposure. Multiple features associated with primary and specialized metabolisms and cell wall biogenesis and maintenance were downregulated by C6-AHL exposure across both datasets. Impacted specialized metabolism features included in biosynthetic gene clusters (BGCs) provided by the BGC prediction platform antiSMASH were further analysed to determine putative role and associated metabolites. A total of six BGCs from *M. xanthus* contained genes impacted by C6-AHL exposure including one core biosynthetic gene (WP_011554909.1) from an annotated thiopeptide/bacteriocin BGC and one regulatory gene (WP_011552861.1) from a putative nonribosomal peptide synthetase-polyketide synthase hybrid BGC (Table S3;

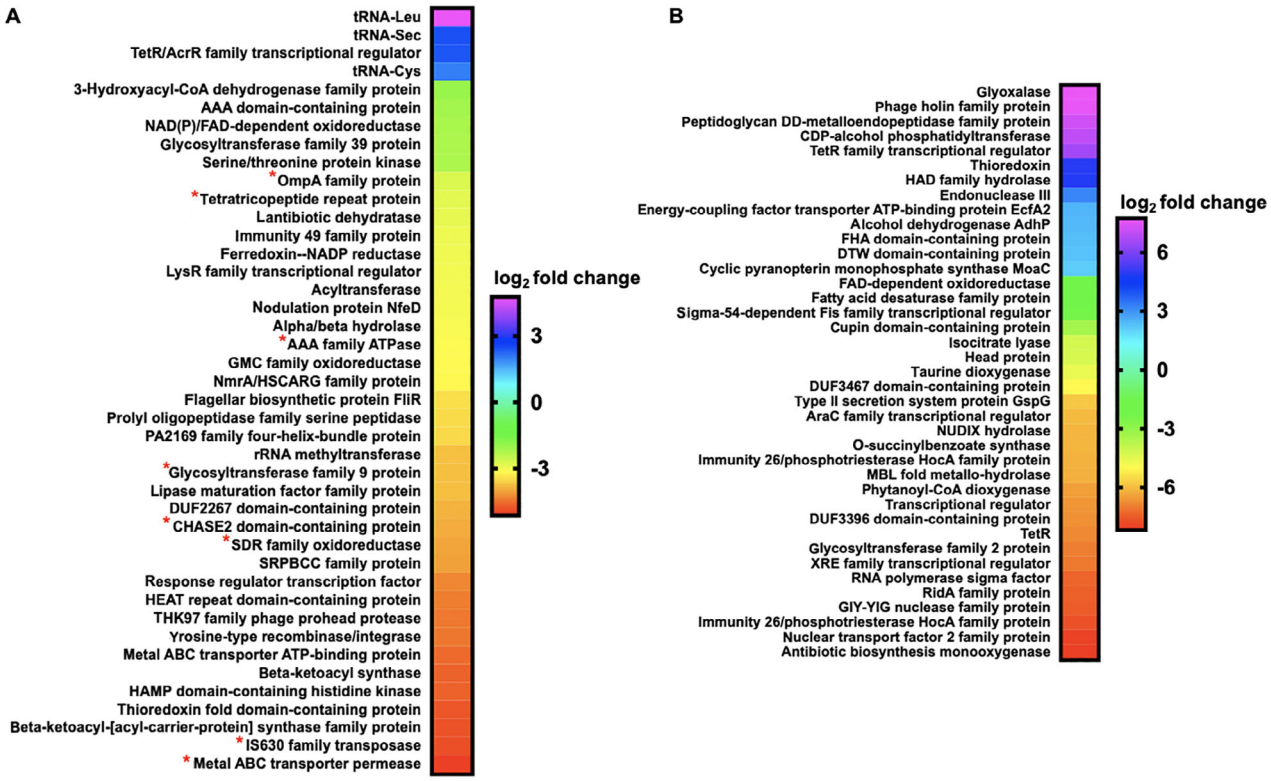

Fig. 1. Transcriptomic data from myxobacteria exposed to C6-AHL.
A. Differentially expressed genes and features from *M. xanthus* exposed to C6-AHL when compared with signal unexposed *M. xanthus* control ($p \leq 0.05$); * indicates features also impacted at $p \leq 0.01$.
B. Differentially expressed genes from *C. ferrugineus* exposed to C6-AHL when compared with signal unexposed *C. ferrugineus* control ($p \leq 0.01$). Data depicted as an average $\log_2$ fold change from three biological replicates. Impacted features annotated as hypothetical not included.

© 2021 The Authors. *Environmental Microbiology* published by Society for Applied Microbiology and John Wiley & Sons Ltd.,

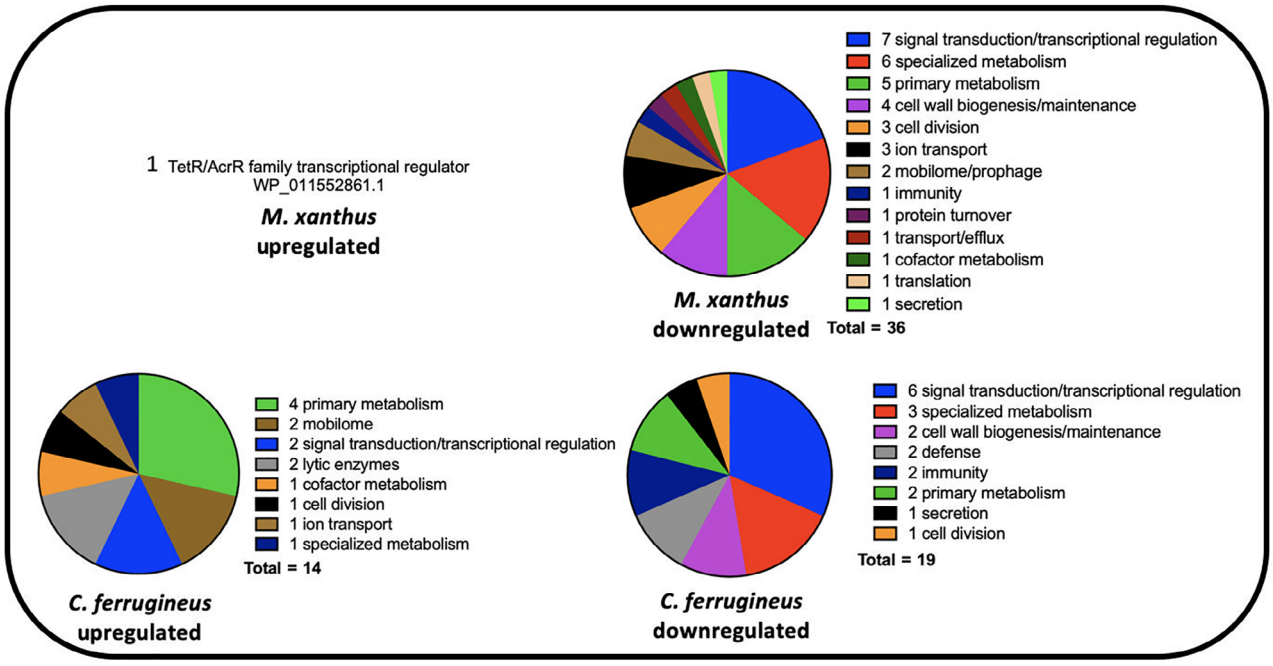

Fig. 2. Putative roles of Prokaryotic Genome Annotation Pipeline (PGAP)-annotated genes impacted by C6-AHL exposure (from Fig. 1) comparing *M. xanthus* and *C. ferrugineus*.

Fig. S1; Blin *et al*., 2021a, 2021b). None of the BGC-associated genes from *M. xanthus* impacted by C6-AHL were from characterized gene clusters with assigned metabolites. A total of 16 BGCs from *C. ferrugineus* included features impacted by C6-AHL exposure, however, no features annotated as core biosynthetic genes, regulatory genes or transport genes were observed (Table S3, Fig. S1).

Considering previous reports that C6-AHL exposure suppresses *M. xanthus* sporulation (Lloyd and Whitworth, 2017), we sought to determine if C6-AHL exposure effected either of the transcriptional regulators associated with *M. xanthus* sporulation FruA or MrpC (Ogawa *et al*., 1996; Robinson *et al*., 2014; Marcos-Torres *et al*., 2020). While no significant change in FruA was observed, transcription of the gene product MrpC was downregulated 1.7-fold by *M. xanthus* exposure to C6-AHL. However, transcription of the FruA (WP_071904077.1) or MrpC (WP_071900118) homologues from *C. ferrugineus* was not significantly changed by C6-AHL exposure. While no obvious predatory features associated with motility or lytic enzymes were directly impacted in our C6-AHL exposed *M. xanthus* results, we suspect that this could be due to the previously reported constitutive toxicity of *M. xanthus* observed in both the presence and absence of prey (Livingstone *et al*., 2018). The increased transcription of lytic enzymes and mobile genetic elements observed from *C. ferrugineus* exposed to C6-AHL suggest a predatory response; however, these features could also be associated with a defence response akin to phage defence. Transcription of neither of the annotated LuxR-type receptors (*M. xanthus*, WP_011555271.1; *C. ferrugineus*, WP_071900454.1) was affected by C6-AHL exposure. Overall considering the most significantly impacted features across both datasets, C6-AHL exposure elicited somewhat similar responses from both myxobacteria including numerous features associated with transcriptional regulation and signal transduction, primary and specialized metabolisms, and cell wall maintenance.

HHQ elicits contrasting responses from M. xanthus *and* C. ferrugineus

Comparative transcriptomics from RNAseq data from exposure experiments with HHQ (9 μM) introduced to plates of *M. xanthus* and *C. ferrugineus* were also conducted in triplicate with DMSO exposures serving as HHQ unexposed, negative controls for comparative analysis. Comparative transcriptomic analysis from RNAseq data revealed HHQ exposure led to a ≥4-fold ($p \leq 0.05$) change in transcription of a total of 186 genes from *C. ferrugineus* and 31 total genes from *M. xanthus* (Fig. 3). Unlike the similar responses elicited by C6-AHL exposure, contrasting responses were apparent when comparing data between the myxobacteria. Data from *M. xanthus* experiments revealed overlap between responses to C6-AHL and HHQ with a total of nine

© 2021 The Authors. *Environmental Microbiology* published by Society for Applied Microbiology and John Wiley & Sons Ltd.,

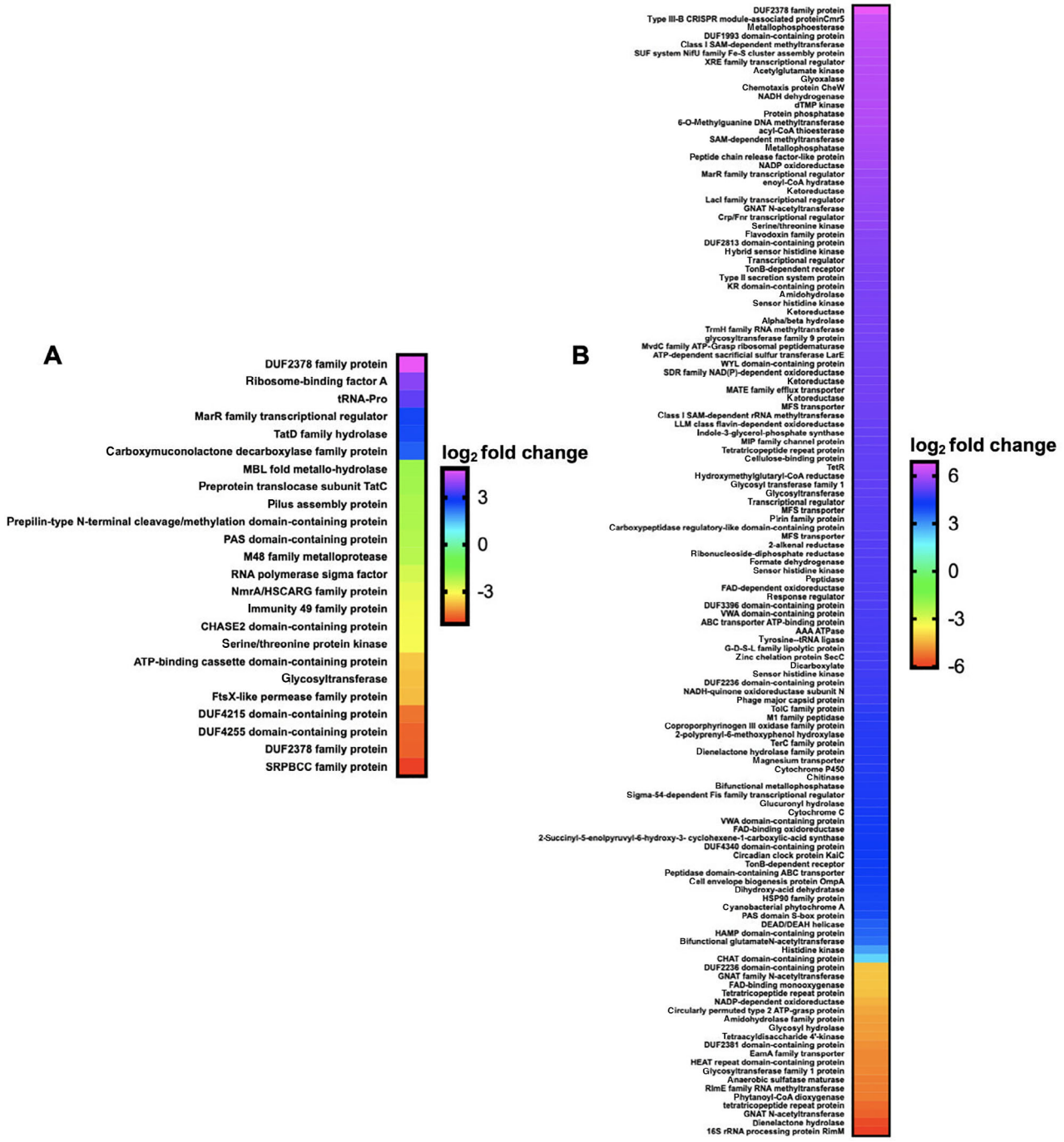

Fig. 3. Transcriptomic data from myxobacteria exposed to HHQ.
A. Differentially expressed genes and features from *M. xanthus* exposed to HHQ when compared with signal unexposed *M. xanthus* control ($p \leq 0.05$).
B. Differentially expressed genes from *C. ferrugineus* exposed to HHQ when compared with signal unexposed *C. ferrugineus* control ($p \leq 0.05$). Data depicted as an average $\log_2$ fold change from three biological replicates. Impacted features annotated as hypothetical not included.

upregulated genes and 22 downregulated genes including five genes also downregulated by C6-AHL exposure. Overlapping annotated features impacted by both C6-AHL and HHQ included a NmrA/HSCARG family protein (WP_011556972.1), an immunity 49 family protein (WP_011550233.1), a CHASE2 domain-containing protein (WP_011554259.1), and two hypothetical proteins (WP_011555268.1 and WP_011552217.1). Comparing

© 2021 The Authors. *Environmental Microbiology* published by Society for Applied Microbiology and John Wiley & Sons Ltd.,

impacted genes from AHL and HHQ exposure experiments, further overlap between putative roles of annotated genes was also observed from *M. xanthus* with multiple impacted genes predicted to be involved in transcriptional regulation and signal transduction and cell wall biogenesis and maintenance (Figs. 2 and 4). Of note, the pleiotropic regulator MrpC was also downregulated 2.2-fold in *M. xanthus* exposed to HHQ which is comparable to 1.7-fold downregulation of MrpC observed with C6-AHL exposure. Only one gene (WP_011554915.1) included in a putative thiopeptide/bacteriocin BGC was significantly impacted by HHQ exposure (Table S3, Fig. S1).

Unlike the overlap in responses to both signals observed from *M. xanthus*, none of the 186 genes effected by HHQ exposure overlapped with the 76 genes impacted by C6-AHL exposure. Considering annotated genes by functional category, *C. ferrugineus* genes upregulated by HHQ exposure (156 total) were largely associated with signal transduction and transcriptional regulation, various metabolic pathways, and multiple genes associated with protein translation and turnover, cell wall biogenesis and maintenance and specialized metabolism were downregulated (29 total; Fig. 4). A total of six BGCs from *C. ferrugineus* contained genes impacted by HHQ exposure. These included three regulatory genes from a nonribosomal peptide synthetase (WP_071896979.1), a type III polyketide synthase (WP_071896419.1), and a linear azol(in)e-containing peptide pathway (WP_071903679.1) as well as a transport-related gene (WP_071904585.1) from a type I polyketide synthase pathway (Table S3, Fig. S1). Interestingly, an annotated FAD-dependent oxidoreductase (WP_071901324.1) homologous to the monooxygenase PsqH from *P. aeruginosa* (91% coverage; 38% identity) which hydroxylates HHQ to yield 2-heptyl-3-hydroxyquinolin-4(1*H*)-one or pseudomonas quinolone signal (PQS) was upregulated 31-fold (Diggle *et al*., 2003; Ritzmann *et al*., 2021). An outlier to the contrasting responses to HHQ, an annotated DUF2378 family protein (*M. xanthus*, WP_011553830.1; *C. ferrugineus*, WP_084736518.1) was significantly upregulated in both myxobacteria; DUF2378 family proteins are ~200 amino acid proteins with no known function that are exclusive to myxobacteria. Overall, these results indicate that *M. xanthus* exhibits a similar transcriptional response to both C6-AHL and HHQ whereas HHQ elicits a distinct response from *C. ferrugineus* dissimilar from the more general response observed from both myxobacteria when exposed to C6-AHL.

Differential metabolic impact of AHL and HHQ signals

Subsequent exposure experiments were conducted with *M. xanthus* and *C. ferrugineus* exactly as done for our RNAseq experiments with an additional AHL signal,

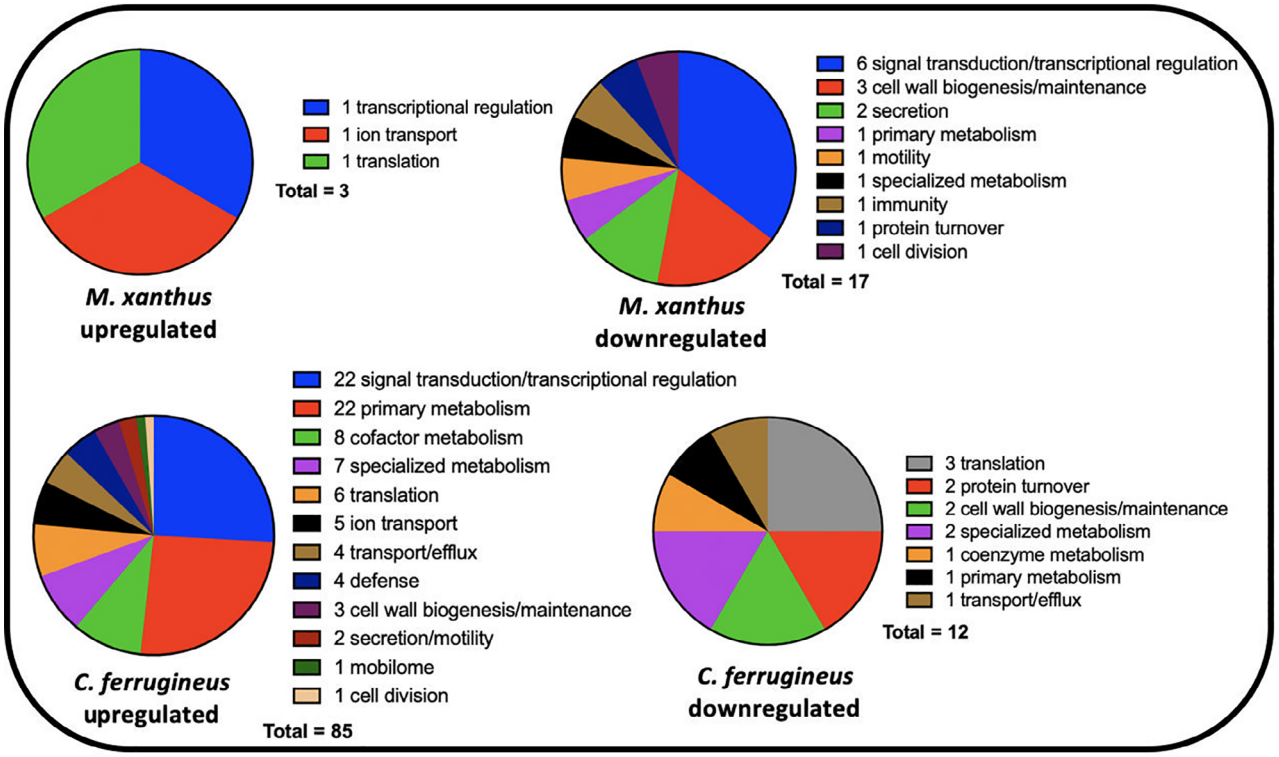

Fig. 4. Putative roles of PGAP-annotated genes impacted by HHQ exposure (from Fig. 3) comparing *M. xanthus* and *C. ferrugineus*.

© 2021 The Authors. *Environmental Microbiology* published by Society for Applied Microbiology and John Wiley & Sons Ltd.,

3-oxo-C6-AHL, also included. Crude, organic phase extracts generated from these experiments were subjected to untargeted mass spectrometry and the XCMS-MRM (v3.7.1) platform (Domingo-Almenara *et al*., 2018; Forsberg *et al*., 2018) was utilized for comparative analysis and determination of statistical significance for all detected features. Comparing features with significantly impacted intensities ($p \leq 0.02$) during these signal exposure experiments, all three signals elicited a more apparent response from *C. ferrugineus* (Fig. 5, Fig. S2). Despite the comparatively diminished response from *M. xanthus*, two general trends were apparent when comparing the signals responses between both myxobacteria. First, C6-AHL and 3-oxo-C6-AHL exposure resulted in highly similar responses from both myxobacteria with few to no uniquely impacted features specific to either AHL signal (Fig. 5). Second, HHQ exposure induced a dramatic change in the metabolic profile of *C. ferrugineus* that was not observed from HHQ-exposed *M. xanthus*. A total of 47 features from *C. ferrugineus* were impacted by both AHL signals while 133 features were affected by HHQ exposure. Intrigued by the difference in responses, additional experiments where both myxobacteria were exposed to exogenous C6-AHL and HHQ simultaneously were done. Comparative analysis of results revealed that the addition of C6-AHL did not dramatically impact the change in metabolic profile observed from either myxobacteria when exposed to HHQ (Fig. 6). Conversely, impacted features observed in our previous AHL exposure experiments were not observed in our C6-AHL + HHQ experiments. For example, of the 47 total overlapping *C. ferrugineus* features with significantly changed intensities during AHL exposure conditions, 36 were not observed to change during C6-AHL + HHQ exposure experiments. The Global Natural Products Social Molecular Networking (GNPS) platform (Wang *et al*., 2016) was used to determine if any impacted features could be associated with characterized metabolites. Although networks included detected features with exact masses for myxovirescin

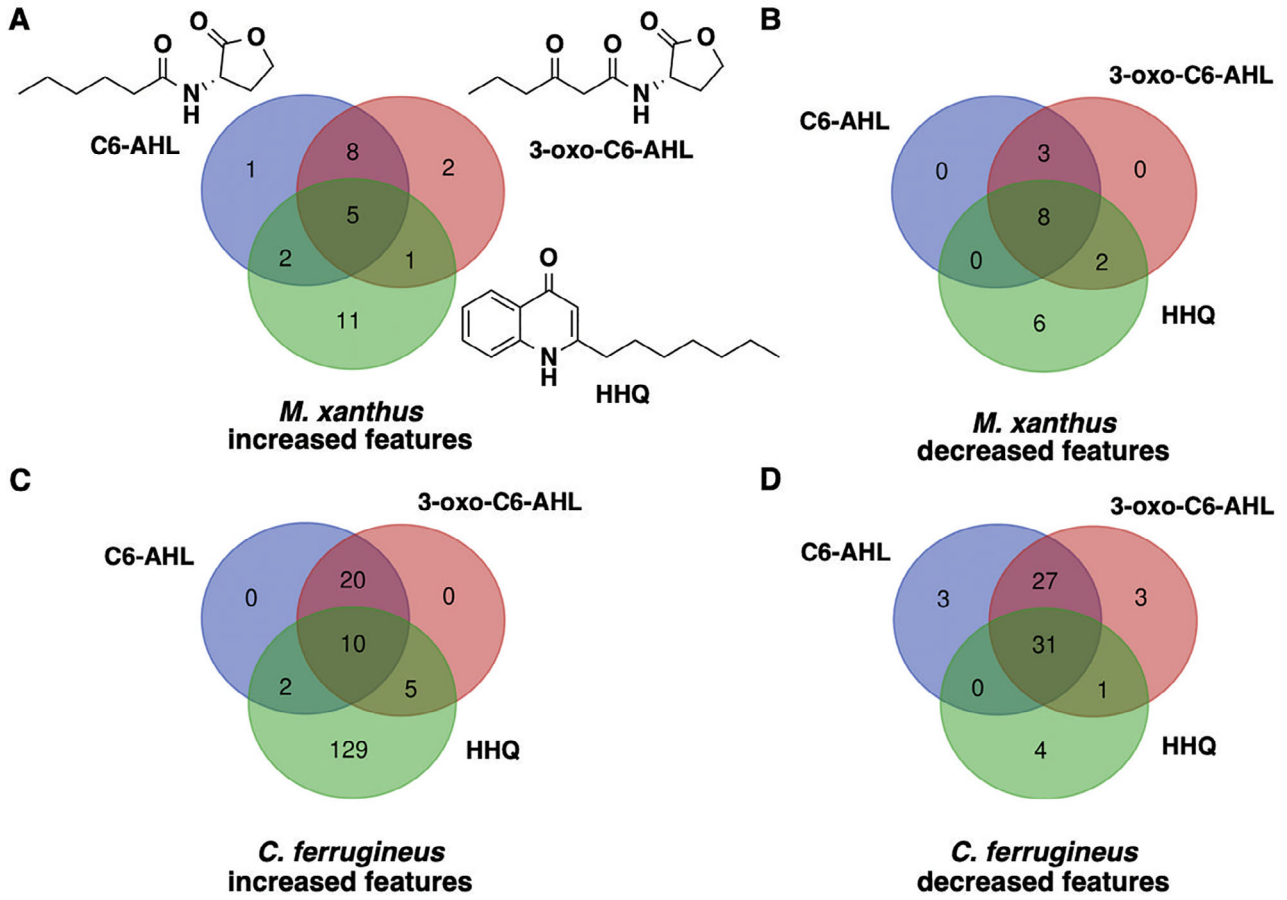

Fig. 5. Comparison of metabolomic response to C6-AHL, 3-oxo-C6-AHL and HHQ exposure experiments with *M. xanthus* (A and B) and *C. ferrugineus* (C and D). Numbers included in each Venn diagram account for a unique detected feature with a significantly impacted intensity upon exposure to the indicated signalling molecule provided by XCMS-multigroup analysis ($n = 3$, $p \leq 0.02$).

© 2021 The Authors. *Environmental Microbiology* published by Society for Applied Microbiology and John Wiley & Sons Ltd.,

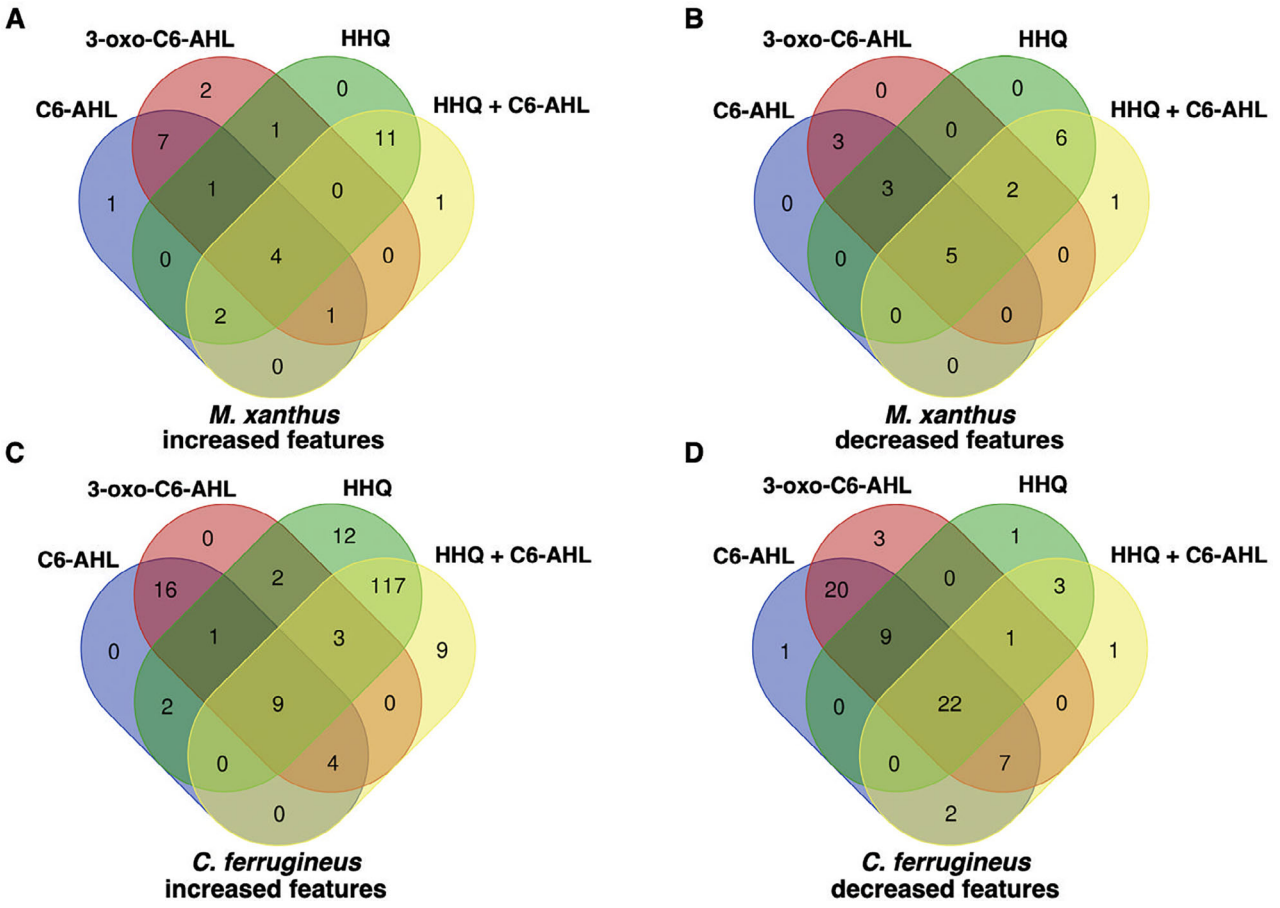

Fig. 6. Comparison of metabolomic response to C6-AHL, 3-oxo-C6-AHL, and HHQ exposure experiments with *M. xanthus* (A and B) and *C. ferrugineus* (C and D) including additional C6-AHL + HHQ exposure experiments. Numbers included in each Venn diagram account for a unique detected feature with a significantly impacted intensity upon exposure to the indicated signalling molecule provided by XCMS-multigroup analysis ($n = 3$, $p \leq 0.02$).

and degraded myxovirescin metabolites were observed in *M. xanthus* extracts and detected features with exact masses for various tubulysins were observed in *C. ferrugineus* extracts (Fig. S3), detected quantities were not impacted by AHL or HHQ exposure. From these results, we determined that both myxobacteria demonstrate a metabolic response unique to either HHQ or AHL-type chemical signals with a conserved response to both C6-AHL and 3-oxo-C6-AHL. These data also revealed a unique metabolic response from *C. ferrugineus* when exposed to HHQ similar to our previous transcriptomic observation.

Conserved metabolomic response to AHLs and determination of core L-homoserine lactone elicitor

Intrigued by the overlap in metabolic responses observed from AHL signal exposure, we were curious if the core homoserine lactone moiety present in all AHL-type quorum signals was sufficient to elicit a similar response. Untargeted mass spectrometry and XCMS-MRM analysis of additional exposure experiments with *C. ferrugineus* including either L-homoserine lactone (L-HSL) the stereoisomer present in natural AHL-type quorum signals (Papenfort and Bassler, 2016; Mukherjee and Bassler, 2019), D-homoserine lactone (D-HSL) the enantiomer of L-HSL, or boiled C6-AHL were completed to determine any overlap with previously observed responses to C6-AHL and 3-oxo-C6-AHL exposure. Comparative analysis of statistically impacted features by signal intensity ($p \leq 0.02$) revealed 20 overlapping features from the L-HSL, C6-AHL, and 3-oxo-C6-AHL exposure experiments and just three overlapping features from the L-HSL, D-HSL, C6-AHL, and 3-oxo-C6-AHL exposure experiments (Fig. 7, Fig. S4). Hierarchical clustering of detected feature intensities from L-HSL, D-HSL, C6-AHL, and control datasets also revealed clustering between L-HSL and C6-AHL datasets (Fig. S5). These

© 2021 The Authors. *Environmental Microbiology* published by Society for Applied Microbiology and John Wiley & Sons Ltd.,

results suggest that the core homoserine lactone core present in all AHLs is sufficient for predatory eavesdropping by myxobacteria.

Oxidative detoxification of HHQ observed from C. ferrugineus

Comparing metabolomic datasets from HHQ exposure experiments, oxidized analogs of HHQ detected at 260.164 m/z were exclusive to the *C. ferrugineus* dataset. Authentic standards for the oxidized HHQ quinolone signals PQS and 2-heptyl-1-hydroxyquinolin-4(1*H*)-one (HQNO) were used to determine that both oxidized signals were present in HHQ-exposed *C. ferrugineus* extracts (Fig. 8; Fig. S6; Cao *et al*., 2020). Oxidative detoxification of quinolone signals including HHQ has been reported from numerous bacteria (Thierbach *et al*., 2017; Ritzmann *et al*., 2021). Additional experiments exposing *C. ferrugineus* to either PQS or HQNO provided insight into a similar oxidative detoxification route for quinolone signals with HHQ observed to be oxidized to either HQNO or PQS. The presence of a metabolite with an exact mass and similar MS^2 fragmentation pattern matching PQS-*N*-oxide (PQS-NO) an oxidation product reported by Thierbach *et al*. was also observed in *C. ferrugineus* extracts from HHQ, PQS, and HQNO exposure experiments suggesting subsequent oxidation of both PQS and HQNO (Fig. 8; Figs. S7 and S8; Thierbach *et al*., 2017). These results suggest that *C. ferrugineus* possesses a detoxification route for quinolone signals not observed from *M. xanthus* and oxidizes the quinolone signals HHQ, PQS, and HQNO.

C. ferrugineus *response to HHQ correlates with superior predation of* P. aeruginosa

Predation assays using the lawn culture method were conducted in triplicate on lawns of *P. aeruginosa* with both *M. xanthus* and *C. ferrugineus* (Morgan *et al*., 2010). These assays confirmed that *P. aeruginosa* was comparatively more susceptible to predation by *C. ferrugineus* (Fig. 9A). Secretion of toxic quinolone signals in soil is thought to provide *P. aeruginosa* an advantage, and HHQ inhibition of soil-dwelling *Bacillus atrophaeus* swarming motility has been observed (Reen *et al*., 2015; Ritzmann *et al*., 2021). Subsequent swarming expansion assays with *M. xanthus* and *C. ferrugineus* on medias with and without supplemented HHQ were done to determine if similar antiswarming activities were observed. From these assays, we observed HHQ (9 μM) significantly inhibited *M. xanthus* swarming but not *C. ferrugineus* swarming (Fig. 9B and C). We suggest oxidative degradation of quinolone signals observed from *C. ferrugineus* contributes to predation of *P. aeruginosa*. Altogether these results indicate the unique response to exogenous HHQ observed from *C. ferrugineus* to be an evolved trait associated with exposure to quinolone signals that correlates with predation of quinolone signal-producing pseudomonads.

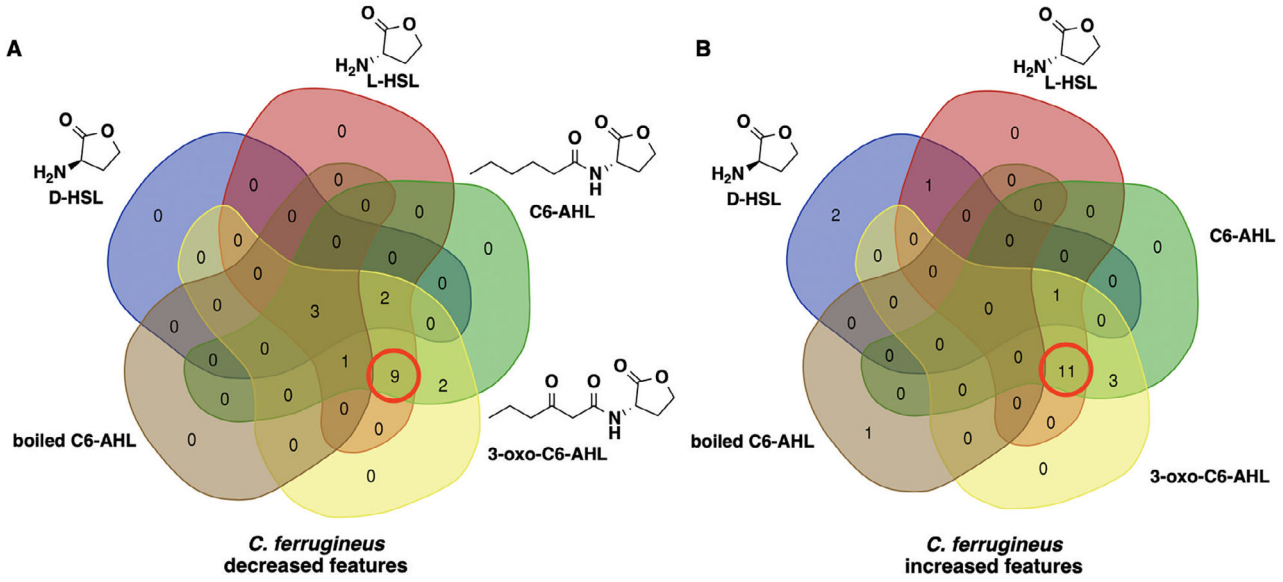

Fig. 7. Overlap in metabolic response to C6-AHL, 3-oxo-C6-AHL and L-HSL exposure observed from *C. ferrugineus*. Venn diagrams include the number of metabolic features with a significant increase (A) or decrease (B) in detected ion intensity compared with signal unexposed controls provided by XCMS-multigroup analysis ($n = 3$; $p \leq 0.02$). Red circles indicate overlapping metabolic features of L-HSL with C6-AHL and 3-oxo-C6-AHL.

© 2021 The Authors. *Environmental Microbiology* published by Society for Applied Microbiology and John Wiley & Sons Ltd.,

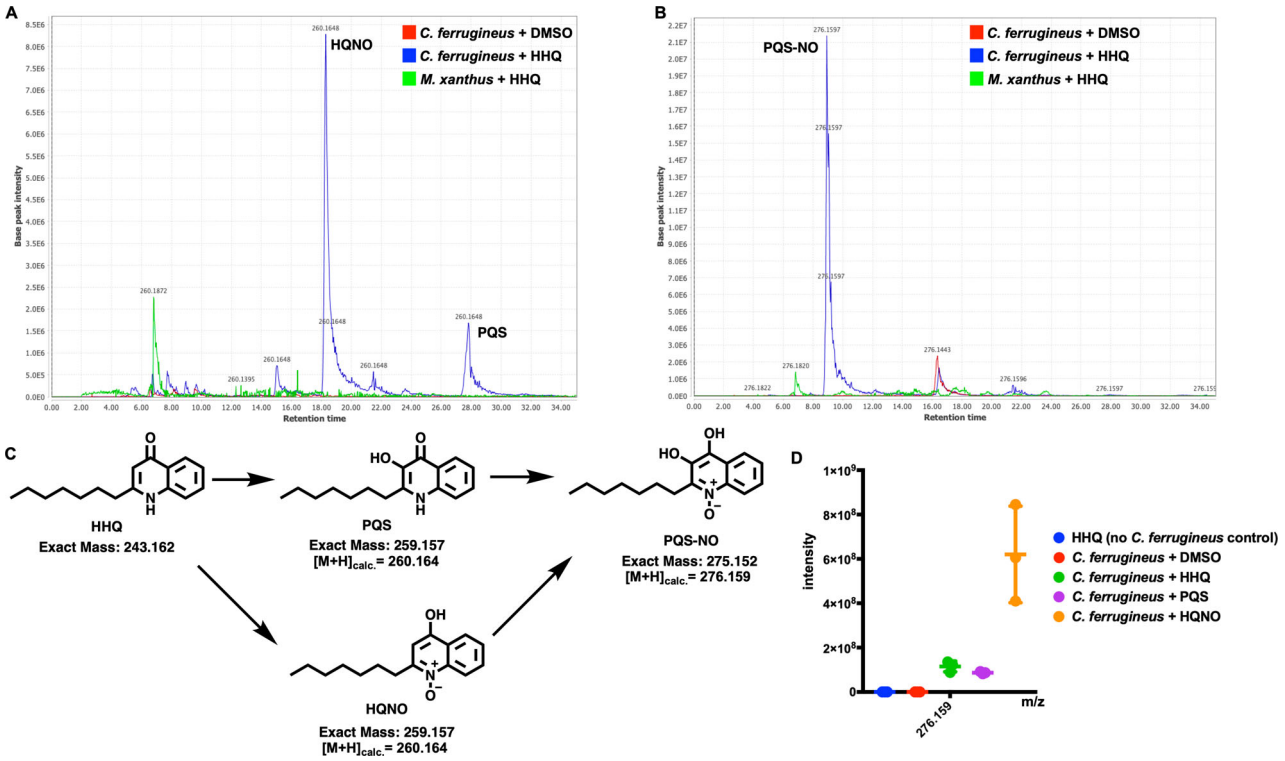

Fig. 8. A. Extracted ion chromatograph (EIC) depicting presence of HQNO and PQS in HHQ exposed extracts from *C. ferrugineus* and not observed in HHQ exposed extracts from *M. xanthus*. B. EIC depicting presence of PQS-NO in HHQ exposed extracts of *C. ferrugineus*, also not present in *M. xanthus* extracts. Chromatographs rendered with MZmine v2.37. C. Oxidative detoxification of HHQ by *C. ferrugineus* including exact mass values from ChemDraw Professional v17.1. D. Detected ion intensities for PQS-NO comparing crude extracts of *C. ferrugineus* exposed to HHQ, PQS and HQNO; detected intensity data provided by XCMS-multigroup analysis ($n = 3$; $p \leq 0.02$).

Discussion

Although the predatory lifestyles of myxobacteria have long been associated with their capacity as a resource for natural products discovery, the chemical ecology of predator–prey interactions remains underexplored (Findlay, 2016; Munoz-Dorado *et al*., 2016; Herrmann *et al*., 2017). The recent discovery that exogenous AHL quorum signals associated with Gram-negative prey bacteria increase the predatory capacity of *M. xanthus* provides an excellent example of shared chemical space within microbial communities influencing predation (Lloyd and Whitworth, 2017). Utilizing comparative transcriptomics and metabolomics, we sought to determine the generality of predatory eavesdropping and how the phenomenon might correlate with prey range by comparing responses from *M. xanthus* and *C. ferrugineus* when exposed to structurally distinct quorum signals associated with the opportunistic pathogen *P. aeruginosa*.

Initial transcriptomic data comparing *M. xanthus* and *C. ferrugineus* exposed to C6-AHL revealed overlapping transcriptional responses from both myxobacteria. Originally referenced as predatory eavesdropping, we sought to determine the impact of C6-AHL on genes with annotations affiliated with predation and predatory responses such as motility features, lytic enzymes and specialized metabolism (Munoz-Dorado *et al*., 2016). Transcription of multiple genes associated with transcriptional regulation, metabolism and cell wall maintenance was influenced by exogenous C6-AHL across both myxobacteria. Although we observed numerous genes embedded in putative specialized metabolite biosynthetic pathways impacted by C6-AHL from both myxobacteria, none were included in the annotated BGCs for myxovirescin or myxoprincomide. Since these are the only two myxobacterial metabolites currently implicated in predation, further investigation is required to determine if C6-AHL induces production of biologically active, specialized metabolites (Xiao *et al*., 2011; Cortina *et al*., 2012; Muller *et al*., 2016; Ellis *et al*., 2019; Wang *et al*., 2019). The only other potential predatory features with a transcriptional response to C6-AHL exposure were putative lytic enzymes from *C. ferrugineus*, and no annotated genes predicted to be involved in motility were affected by C6-AHL in either myxobacteria. Considering the original observation that AHLs stimulate predation by increasing the vegetative population of *M. xanthus*, we suggest

© 2021 The Authors. *Environmental Microbiology* published by Society for Applied Microbiology and John Wiley & Sons Ltd.,

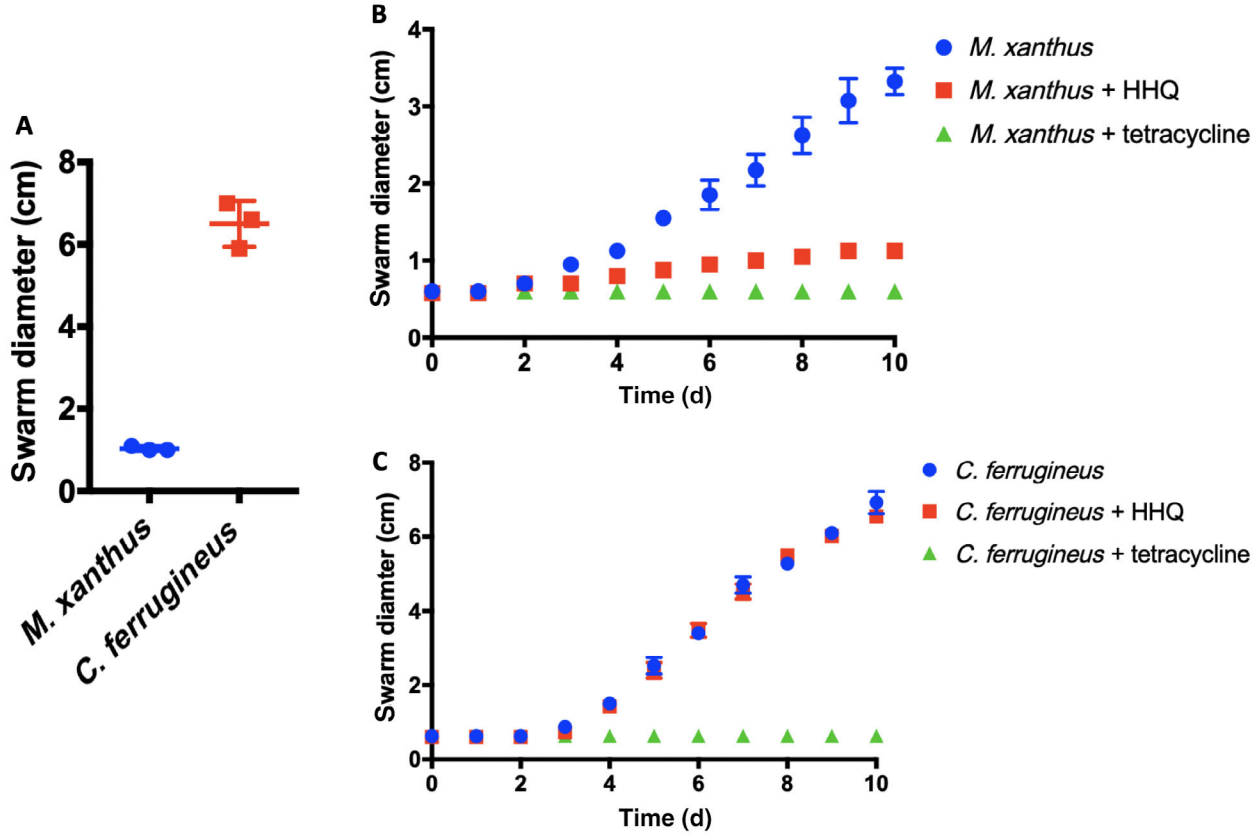

Fig. 9. A. Lawn culture predation assay data depicting superior predation of *P. aeruginosa* by *C. ferrugineus* ($n = 3$; $p \leq 0.005$). Statistical significance calculated using an unpaired t test with Welch's correction. B. Swarming expansion assay data depicting HHQ inhibition of *M. xanthus* swarming ($n = 4$) with significant differences in swarm diameters ($p < 0.001$) observed between HHQ exposed and unexposed data after day 3. C. Swarming expansion assay data depicting no significant inhibition of *C. ferrugineus* swarming ($n = 4$) during HHQ exposure conditions. Statistical significance for swarming assays was determined using two-way ANOVA and Tukey's multiple comparisons test.

that the observed change in transcription of genes associated with metabolism and signal transduction from both myxobacteria may correspond with a similar population-based response and shift in vegetative state (Lloyd and Whitworth, 2017). The decreased transcription of the gene encoding for MrpC, a developmental regulator involved in sporulation (Robinson *et al*., 2014), observed in our *M. xanthus* dataset also supports a population-based response to C6-AHL.

Subsequent comparative metabolomics experiments indicated that C6-AHL and 3-oxo-C6-AHL elicit overlapping responses from both myxobacteria and that the core AHL moiety L-HSL also elicits a similar response from *C. ferrugineus*. We conclude that the overlap between C6-AHL, 3-oxo-C6-AHL and L-HSL indicates an evolved recognition of the homoserine lactone unit present in all AHL quorum signals (Papenfort and Bassler, 2016; Mukherjee and Bassler, 2019). As generalist predators, a more general process for AHL perception that responds to a core moiety in the scaffold of AHLs might be preferred to a specialized process associated with the variable *N*-acylamides of AHLs. We also suspect this centralized response to L-HSL may relate to the absence of a LuxR-type AHL receptor that includes a conserved AHL-binding domain. The ubiquity of AHL quorum signals amongst Gram-negative bacteria combined with the overlap in observed responses from *M. xanthus* and *C. ferrugineus* suggest that AHL-based eavesdropping by myxobacteria could be a general trait that benefits predation.

Unlike the overlap in responses to AHL exposure, the quinolone signal HHQ elicited a contrasting transcriptomic from *M. xanthus* and *C. ferrugineus*. Contrary to *M. xanthus*, *C. ferrugineus* upregulated genes associated with signal transduction and transcriptional regulation, various metabolic pathways, and multiple genes associated with protein translation and turnover, cell wall biogenesis and maintenance, and specialized metabolism when exposed to HHQ. Interestingly, an annotated FAD-dependent oxidoreductase homologous to the

© 2021 The Authors. *Environmental Microbiology* published by Society for Applied Microbiology and John Wiley & Sons Ltd.,

monooxygenase PqsH from *P. aeruginosa*, which hydroxylates HHQ to yield PQS was upregulated 31-fold in *C. ferrugineus* exposed to HHQ. Subsequent metabolomic experiments confirmed the presence of two oxidized analogs of HHQ, PQS and HQNO (Dubern and Diggle, 2008; Thierbach *et al*., 2017). The detection of these oxidized quinolones as well as an additional feature, PQS-NO, previously associated with the oxidative detoxification of quinolone signals in HHQ exposed *C. ferrugineus* samples and absence in *M. xanthus* samples suggests that *M. xanthus* is unable to similarly metabolize HHQ (Dubern and Diggle, 2008; Thierbach *et al*., 2017; Ritzmann *et al*., 2021). Oxidative detoxification of quinolone signals produced by pseudomonads has previously been reported from strains of *Arthrobacter*, *Rhodococcus* and *Staphylococcus aureus* (Thierbach *et al*., 2017). Subsequent swarming expansion assays revealed HHQ inhibits *M. xanthus* swarming but not *C. ferrugineus* swarming. We suggest that this oxidative detoxification process contributes to the superior predation of *P. aeruginosa* observed from *C. ferrugineus* in our predation assays comparing both myxobacteria.

Despite being considered keystone taxa within microbial communities (Petters *et al*., 2021), the extent of myxobacterial bacterivory and its contribution to nutrient cycling within microbial food webs remains unknown. These results further demonstrate myxobacterial eavesdropping on prey signalling molecules and provide insight into how responses to exogenous signals might correlate with prey range of myxobacteria. Although broadly considered generalist predators, predatory specialization has been observed from myxobacteria. Oxidation of quinolone signals and superior predation of *P. aeruginosa* observed from *C. ferrugineus* provides an example of how prey signalling molecules and the shared chemical ecology of microbial communities influence myxobacterial predation.

Experimental procedures

Cultivation of M. xanthus and C. ferrugineus

Cystobacter ferrugineus strain Cbfe23, DSM 52764, initially obtained from German Collection of Microorganisms (DSMZ) in Braunschweig, and *Myxococcus xanthus* strain GJV1 were employed in this study. *Cystobacter ferrugineus* was grown on VY/2 agar (5 g l^{-1} baker's yeast, 1.36 g l^{-1} $CaCl_2$, 0.5 mg l^{-1} vitamin B12, 15 g l^{-1} agar, pH 7.2). Whereas, CTTYE agar (1.4% w/v agar, 1% Casitone, 10 mM Tris–HCl (pH 7.6), 1 mM potassium phosphate (pH 7.6), 8 mM $MgSO_4$, 0.5% yeast extract) was utilized to culture *M. xanthus*.

Quorum signal exposure experiments

For signal exposure conditions, required volumes for 9 μM of filter sterilized, HHQ (Sigma), C6-AHL (Cayman Chemical), 3-oxo-C6-AHL (Cayman Chemical), L-HSL (Cayman Chemical), D-HSL (Cayman Chemical), PQS (Sigma) and HQNO (Sigma) from a 150 mM stock prepared in DMSO were added to autoclaved medium at 55°C. Boiled AHL samples were prepared according to established methodology (Lloyd and Whitworth, 2017). For RNA-seq and LC–MS/MS analysis, *C. ferrugineus* was cultivated on VY/2 agar medium, and *M. xanthus* was cultured on CTTYE agar medium. For all signal exposure experiments both myxobacteria were grown at 30°C with *C. ferrugineus* grown for 10 days and *M. xanthus* grown 14 days.

RNA sequencing experiments and analysis

Myxobacterial cells were scrapped from the agar plates and stored in RNA-ladder. Total RNA was isolated from the samples using the RNeasy PowerSoil Total RNA Kit (Qiagen) following the manufacturer's instructions. Consistent aliquots of biomass (500 mg) from each myxobacteria were used for RNA extractions. The concentration of total RNA was determined using the Qubit RNA Assay Kit (Life Technologies). For rRNA depletion, first, 1000 ng of total RNA was used to remove the DNA contamination using Baseline-ZERO DNase (Epicentre) following the manufacturer's instructions followed by purification using the RNA Clean and Concentrator-5 columns (Zymo Research). DNA free RNA samples were used for rRNA removal by using RiboMinus rRNA Removal Kit (Bacteria; Thermo Fisher Scientific) and final purification was performed using the RNA Clean and Concentrator-5 columns (Zymo Research). rRNA depleted samples were used for library preparation using the KAPA mRNA HyperPrep Kits (Roche) by following the manufacturer's instructions. Following the library preparation, the final concentration of each library was measured using the Qubit dsDNA HS Assay Kit (Life Technologies), and average library size for each was determined using the Agilent 2100 Bioanalyzer (Agilent Technologies; Tables S1 and S2). The libraries were then pooled in equimolar ratios of 0.75 nM, and sequenced paired end for 300 cycles using the NovaSeq 6000 system (Illumina). RNA sequencing was conducted by MR DNA (Molecular Research LP). RNAseq analysis was performed using ArrayStar V15 and the R-package DESeq2 for differential expression data. Raw data from RNAseq analysis publicly available at the National Centre for Biotechnology Information Sequence Read Archive under the following BioProjects PRJNA555507, PRJNA730806 and PRJNA730808.

© 2021 The Authors. *Environmental Microbiology* published by Society for Applied Microbiology and John Wiley & Sons Ltd.,

AntiSMASH analysis

Biosynthetic gene clusters from *M. xanthus* DK1622 deposited in the antiSMASH database version 3 (Blin *et al*., 2021b) were used in our analysis of specialized metabolite genes included in BGCs. The .gbk file for the *C. ferrugineus* genome sequence deposited at NCBI (NZ_MPIN00000000.1) was analysed with antiSMASH version 6 (Blin *et al*., 2021a) to determine BGCs and identify included specialized metabolite genes. All BGC-associated genes resulting from these analyses are provided in Table S3.

Organic phase extraction of metabolites

After cultivation, myxobacterial plates were manually diced and extracted with excess EtOAc. Pooled EtOAc was filtered and dried *in vacuo* to provide crude extracts for LC–MS/MS analysis. LC–MS/MS analysis of the extracted samples was performed on an Orbitrap Fusion instrument (Thermo Scientific, San Jose, California) controlled with Xcalibur version 2.0.7 and coupled to a Dionex Ultimate 3000 nanoUHPLC system. Samples were loaded onto a PepMap 100 C18 column (0.3 mm $\times$ 150 mm, 2 μm, Thermo Fisher Scientific). Separation of the samples was performed using mobile phase A (0.1% formic acid in water) and mobile phase B (0.1% formic acid in acetonitrile) at a rate of 6 μl min^{-1}. The samples were eluted with a gradient consisting of 5% to 60% solvent B over 15 min, ramped to 95% B over 2 min, held for 3 min, and then returned to 5% B over 3 min and held for 8 min. All data were acquired in positive ion mode. Collision induced dissociation (CID) was used to fragment molecules, with an isolation width of 3 m z^{-1} units. The spray voltage was set to 3600 V, and the temperature of the heated capillary was set to 300°C. In CID mode, full MS scans were acquired from m/z 150 to 1200 followed by eight subsequent MS^2 scans on the top eight most abundant peaks. The nominal orbitrap resolution for both the MS^1 and MS^2 scans was 60,000. The expected mass accuracy based on external calibration was <3 ppm. MZmine 2.53 was used to generate extracted ion chromatograms (Pluskal *et al*., 2010). Organic phase extraction was utilized in combination with a lower mass range cutoff of 150 m z^{-1} to minimize detected primary metabolites and effectively prioritize analysis of less polar, higher mass specialized metabolites.

XCMS analysis

Generated data were converted to .mzXML files using MS-Convert (Adusumilli and Mallick, 2017). Multigroup analysis of converted .mzXML files was done using XCMS-MRM and the default HPLC/Orbitrap parameters (Domingo-Almenara *et al*., 2018; Forsberg *et al*., 2018). Within the XCMS-MRM result tables, determination of signal-impacted detected features was afforded by filtering results for those with a $p \leq 0.02$.

GNPS analysis

Converted .mzXML files were used to generate mass spectrometry molecular networks using the GNPS platform release 28.2 (Wang *et al*., 2016). All included LC–MS/MS data were deposited as a publicly available MassIVE dataset (MSV000087999).

Lawn culture predation assays

Pseudomonas aeruginosa ATCC 10145^T was purchased from the American Type Culture Collection (ATCC). The predation experiment was performed according to (Pham *et al*., 2005; Morgan *et al*., 2010). Briefly, an overnight grown culture of *P. aeruginosa* was pelleted at 5000 x g. The cell pellet was washed with TM buffer and pelleted again. The pelleted cells were resuspended in TM buffer to an OD_{600} 0.5. A 250 μl volume of resuspended cell suspension was utilized to make a uniform bacterial lawn on a WAT agar plate. Myxobacterium *M. xanthus* GJV1 was grown on CTTYE agar, and *C. ferrugineus* was grown on VY/2 agar for 7 days. A 600 mm^2 agar block of each myxobacteria was excised and placed at the centre of the *P. aeruginosa* cell lawn. Assays were incubated at 30°C and swarm diameters measured after 4 days.

Swarming expansion assays

Swarming expansion assays were performed using modified established methods (Lloyd and Whitworth, 2017). Myxobacteria were grown on either VY/2 or CTTYE agar media as previously described for 4 days at 30°C. A homogenous bacterial suspension was created using sterile distilled water, vortexed, and equal to an OD_{600} 0.5 for *C. ferrugineus* and an OD_{600} 1.0 for *M. xanthus*. Then 5 μl of myxobacterial suspension was aliquoted within the centre of 100 mm $\times$ 15 mm plates supplemented within respective medias with either 9 μM filter sterilized HHQ (Sigma), without HHQ, or supplemented with 34 μM filter sterilized tetracycline (Thermo Fisher Scientific). Conditions without HHQ and tetracycline were used as controls. Swarming diameters (cm) were assessed and recorded daily for 10 days.

PRISM v7.0d was used to measure the statistical significance of changes in swarm expansion rates across the strains using two-way ANOVA and the Tukey's multiple comparisons test.

© 2021 The Authors. *Environmental Microbiology* published by Society for Applied Microbiology and John Wiley & Sons Ltd.,

ACKNOWLEDGEMENTS

The authors appreciate funding and support from the National Institute of Allergy and Infectious Diseases (R15AI137996). Research reported in this publication was supported by an Institutional Development Award (IDeA) from the National Institute of General Medical Sciences of the National Institutes of Health under award number P20GM130460. The authors also appreciate Dr. Peter Zee for providing us with *M. xanthus* strain GJV1.

References

Adusumilli, R., and Mallick, P. (2017) Data conversion with ProteoWizard msConvert. *Methods Mol Biol* **1550**: 339–368.

Akbar, S., Dowd, S.E., and Stevens, D.C. (2017) Draft genome sequence of *Cystobacter ferrugineus* strain Cbfe23. *Genome Announc* **5**: e01601-16.

Albataineh, H., Duke, M., Misra, S.K., Sharp, J.S., and Stevens, D.C. (2021) Identification of a solo acylhomoserine lactone synthase from the myxobacterium *Archangium gephyra*. *Sci Rep* **11**: 3018.

Arend, K.I., Schmidt, J.J., Bentler, T., Luchtefeld, C., Eggerichs, D., Hexamer, H.M., and Kaimer, C. (2020) *Myxococcus xanthus* predation of gram-positive or gram-negative bacteria is mediated by different bacteriolytic mechanisms. *Appl Environ Microbiol* **87**: e02382-20.

Baikalov, I., Schroder, I., Kaczor-Grzeskowiak, M., Grzeskowiak, K., Gunsalus, R.P., and Dickerson, R.E. (1996) Structure of the *Escherichia coli* response regulator NarL. *Biochemistry* **35**: 11053–11061.

Baltz, R.H. (2019) Natural product drug discovery in the genomic era: realities, conjectures, misconceptions, and opportunities. *J Ind Microbiol Biotechnol* **46**: 281–299.

Cao, T., Sweedler, J.V., Bohn, P.W., and Shrout, J.D. (2020) Spatiotemporal distribution of *Pseudomonas aeruginosa* alkyl quinolones under metabolic and competitive stress. *mSphere*: **5**, e00426-20.

Blin, K., Shaw, S., Kloosterman, A.M., Charlop-Powers, Z., van Wenzel, G.P., Medema, M.H., and Weber, T. (2021b) antiSMASH 6.0: improving cluster detection and comparison capabilities. *Nucleic Acids Res* **49**: W29–W35.

Blin, K., Shaw, S., Kautsar, S.A., Medema, M.H., and Weber, T. (2021a) The antiSMASH database version 3: increased taxonomic coverage and new query features for modular enzymes. *Nucleic Acids Res* **49**: D639–D643.

Cortina, N.S., Krug, D., Plaza, A., Revermann, O., and Müller, R. (2012) Myxoprincomide: a natural product from *Myxococcus xanthus* discovered by comprehensive analysis of the secondary metabolome. *Angew Chem Int Ed Engl* **51**: 811–816.

Deziel, E., Lepine, F., Milot, S., He, J., Mindrinos, M.N., Tompkins, R.G., and Rahme, L.G. (2004) Analysis of *Pseudomonas aeruginosa* 4-hydroxy-2-alkylquinolines (HAQs) reveals a role for 4-hydroxy-2-heptylquinoline in cell-to-cell communication. *Proc Natl Acad Sci U S A* **101**: 1339–1344.

Diggle, S.P., Winzer, K., Chhabra, S.R., Worrall, K.E., Camara, M., and Williams, P. (2003) The *Pseudomonas aeruginosa* quinolone signal molecule overcomes the cell density-dependency of the quorum sensing hierarchy, regulates rhl-dependent genes at the onset of stationary phase and can be produced in the absence of LasR. *Mol Microbiol* **50**: 29–43.

Domingo-Almenara, X., Montenegro-Burke, J.R., Ivanisevic, J., Thomas, A., Sidibe, J., Teav, T., *et al*. (2018) XCMS-MRM and METLIN-MRM: a cloud library and public resource for targeted analysis of small molecules. *Nat Methods* **15**: 681–684.

Dubern, J.F., and Diggle, S.P. (2008) Quorum sensing by 2-alkyl-4-quinolones in *Pseudomonas aeruginosa* and other bacterial species. *Mol Biosyst* **4**: 882–888.

Ellis, B.M., Fischer, C.N., Martin, L.B., Bachmann, B.O., and McLean, J.A. (2019) Spatiochemically profiling microbial interactions with membrane scaffolded desorption electrospray ionization-ion mobility-imaging mass spectrometry and unsupervised segmentation. *Anal Chem* **91**: 13703–13711.

Findlay, B.L. (2016) The chemical ecology of predatory soil bacteria. *ACS Chem Biol* **11**: 1502–1510.

Forsberg, E.M., Huan, T., Rinehart, D., Benton, H.P., Warth, B., Hilmers, B., and Siuzdak, G. (2018) Data processing, multi-omic pathway mapping, and metabolite activity analysis using XCMS online. *Nat Protoc* **13**: 633–651.

Galloway, W.R., Hodgkinson, J.T., Bowden, S.D., Welch, M., and Spring, D.R. (2011) Quorum sensing in gram-negative bacteria: small-molecule modulation of AHL and AI-2 quorum sensing pathways. *Chem Rev* **111**: 28–67.

Garcia-Reyes, S., Soberon-Chavez, G., and Cocotl-Yanez, M. (2020) The third quorum-sensing system of *Pseudomonas aeruginosa*: Pseudomonas quinolone signal and the enigmatic PqsE protein. *J Med Microbiol* **69**: 25–34.

Goes, A., Lapuhs, P., Kuhn, T., Schulz, E., Richter, R., Panter, F., *et al*. (2020) Myxobacteria-derived outer membrane vesicles: potential applicability against intracellular infections. *Cells*: **9**: 194.

Herrmann, J., Fayad, A.A., and Müller, R. (2017) Natural products from myxobacteria: novel metabolites and bioactivities. *Nat Prod Rep* **34**: 135–160.

Islam, S.T., Vergara Alvarez, I., Saidi, F., Guiseppi, A., Vinogradov, E., Sharma, G., *et al*. (2020) Modulation of bacterial multicellularity via spatio-specific polysaccharide secretion. *PLoS Biol* **18**: e3000728.

Livingstone, P.G., Morphew, R.M., and Whitworth, D.E. (2017) Myxobacteria are able to prey broadly upon clinically-relevant pathogens, exhibiting a prey range which cannot be explained by phylogeny. *Front Microbiol* **8**: 1593.

Livingstone, P.G., Millard, A.D., Swain, M.T., and Whitworth, D.E. (2018) Transcriptional changes when *Myxococcus xanthus* preys on *Escherichia coli* suggest myxobacterial predators are constitutively toxic but regulate their feeding. *Microb Genom* **4**: e000152.

Lloyd, D.G., and Whitworth, D.E. (2017) The myxobacterium *Myxococcus xanthus* can sense and respond to the quorum signals secreted by potential prey organisms. *Front Microbiol* **8**: 439.

Marcos-Torres, F.J., Volz, C., and Müller, R. (2020) An ambruticin-sensing complex modulates *Myxococcus*

© 2021 The Authors. *Environmental Microbiology* published by Society for Applied Microbiology and John Wiley & Sons Ltd.,

xanthus development and mediates myxobacterial interspecies communication. *Nat Commun* **11**: 5563.

Mercier, R., Bautista, S., Delannoy, M., Gibert, M., Guiseppi, A., Herrou, J., *et al*. (2020) The polar Ras-like GTPase MglA activates type IV pilus via SgmX to enable twitching motility in *Myxococcus xanthus*. *Proc Natl Acad Sci U S A* **117**: 28366–28373.

Morgan, A.D., MacLean, R.C., Hillesland, K.L., and Velicer, G.J. (2010) Comparative analysis of myxococcus predation on soil bacteria. *Appl Environ Microbiol* **76**: 6920–6927.

Mukherjee, S., and Bassler, B.L. (2019) Bacterial quorum sensing in complex and dynamically changing environments. *Nat Rev Microbiol* **17**: 371–382.

Muller, S., Strack, S.N., Ryan, S.E., Shawgo, M., Walling, A., Harris, S., *et al*. (2016) Identification of functions affecting predator-prey interactions between *Myxococcus xanthus* and *Bacillus subtilis*. *J Bacteriol* **198**: 3335–3344.

Munoz-Dorado, J., Marcos-Torres, F.J., Garcia-Bravo, E., Moraleda-Munoz, A., and Perez, J. (2016) Myxobacteria: moving, killing, feeding, and surviving together. *Front Microbiol* **7**: 781.

Nair, R.R., Vasse, M., Wielgoss, S., Sun, L., Yu, Y.N., and Velicer, G.J. (2019) Bacterial predator-prey coevolution accelerates genome evolution and selects on virulence-associated prey defences. *Nat Commun* **10**: 4301.

Ogawa, M., Fujitani, S., Mao, X., Inouye, S., and Komano, T. (1996) FruA, a putative transcription factor essential for the development of *Myxococcus xanthus*. *Mol Microbiol* **22**: 757–767.

Papenfort, K., and Bassler, B.L. (2016) Quorum sensing signal-response systems in gram-negative bacteria. *Nat Rev Microbiol* **14**: 576–588.

Perez, J., Contreras-Moreno, F.J., Marcos-Torres, F.J., Moraleda-Munoz, A., and Munoz-Dorado, J. (2020) The antibiotic crisis: how bacterial predators can help. *Comput Struct Biotechnol J* **18**: 2547–2555.

Petters, S., Gross, V., Sollinger, A., Pichler, M., Reinhard, A., Bengtsson, M.M., and Urich, T. (2021) The soil microbial food web revisited: predatory myxobacteria as keystone taxa? *ISME J* **15**: 2665–2675.

Pham, V.D., Shebelut, C.W., Diodati, M.E., Bull, C.T., and Singer, M. (2005) Mutations affecting predation ability of the soil bacterium *Myxococcus xanthus*. *Microbiology (Reading)* **151**: 1865–1874.

Pluskal, T., Castillo, S., Villar-Briones, A., and Oresic, M. (2010) MZmine 2: modular framework for processing, visualizing, and analyzing mass spectrometry-based molecular profile data. *BMC Bioinformatics* **11**: 395.

Reen, F.J., Shanahan, R., Cano, R., O'Gara, F., and McGlacken, G.P. (2015) A structure activity-relationship study of the bacterial signal molecule HHQ reveals swarming motility inhibition in *Bacillus atrophaeus*. *Org Biomol Chem* **13**: 5537–5541.

Reen, F.J., Mooij, M.J., Holcombe, L.J., McSweeney, C.M., McGlacken, G.P., Morrissey, J.P., and O'Gara, F. (2011) The Pseudomonas quinolone signal (PQS), and its precursor HHQ, modulate interspecies and interkingdom behaviour. *FEMS Microbiol Ecol* **77**: 413–428.

Rendueles, O., and Velicer, G.J. (2020) Hidden paths to endless forms most wonderful: complexity of bacterial motility shapes diversification of latent phenotypes. *BMC Evol Biol* **20**: 145.

Ritzmann, N.H., Drees, S.L., and Fetzner, S. (2021) Signal synthase-type versus catabolic monooxygenases: retracing 3-hydroxylation of 2-alkylquinolones and their N-oxides by *Pseudomonas aeruginosa* and other pulmonary pathogens. *Appl Environ Microbiol* **87**: e02241-20.

Robinson, M., Son, B., Kroos, D., and Kroos, L. (2014) Transcription factor MrpC binds to promoter regions of hundreds of developmentally-regulated genes in *Myxococcus xanthus*. *BMC Genomics* **15**: 1123.

Sharma, G., Yao, A.I., Smaldone, G.T., Liang, J., Long, M., Facciotti, M.T., and Singer, M. (2021) Global gene expression analysis of the *Myxococcus xanthus* developmental time course. *Genomics* **113**: 120–134.

Shiner, E.K., Rumbaugh, K.P., and Williams, S.C. (2005) Inter-kingdom signaling: deciphering the language of acyl homoserine lactones. *FEMS Microbiol Rev* **29**: 935–947.

Subramoni, S., and Venturi, V. (2009) LuxR-family 'solos': bachelor sensors/regulators of signalling molecules. *Microbiology (Reading)* **155**: 1377–1385.

Sutton, D., Livingstone, P.G., Furness, E., Swain, M.T., and Whitworth, D.E. (2019) Genome-wide identification of myxobacterial predation genes and demonstration of formaldehyde secretion as a potentially predation-resistant trait of *Pseudomonas aeruginosa*. *Front Microbiol* **10**: 2650.

Sydney, N., Swain, M.T., So, J.M.T., Hoiczyk, E., Tucker, N. P., and Whitworth, D.E. (2021) The genetics of prey susceptibility to myxobacterial predation: A review, including an investigation into *Pseudomonas aeruginosa* mutations affecting predation by *Myxococcus xanthus*. *Microb Physiol* **31**: 1–10.

Thierbach, S., Birmes, F.S., Letzel, M.C., Hennecke, U., and Fetzner, S. (2017) Chemical modification and detoxification of the *Pseudomonas aeruginosa* toxin 2-heptyl-4-hydroxyquinoline N-oxide by environmental and pathogenic bacteria. *ACS Chem Biol* **12**: 2305–2312.

Thiery, S., and Kaimer, C. (2020) The predation strategy of *Myxococcus xanthus*. *Front Microbiol* **11**: 2.

Tobias, N.J., Brehm, J., Kresovic, D., Brameyer, S., Bode, H.B., and Heermann, R. (2020) New vocabulary for bacterial communication. *Chembiochem* **21**: 759–768.

Vannini, A., Volpari, C., Gargioli, C., Muraglia, E., Cortese, R., De Francesco, R., *et al*. (2002) The crystal structure of the quorum sensing protein TraR bound to its autoinducer and target DNA. *EMBO J* **21**: 4393–4401.

Wade, D.S., Calfee, M.W., Rocha, E.R., Ling, E.A., Engstrom, E., Coleman, J.P., and Pesci, E.C. (2005) Regulation of pseudomonas quinolone signal synthesis in *Pseudomonas aeruginosa*. *J Bacteriol* **187**: 4372–4380.

Wang, C., Liu, X., Zhang, P., Wang, Y., Li, Z., Li, X., *et al*. (2019) *Bacillus licheniformis* escapes from *Myxococcus xanthus* predation by deactivating myxovirescin A through enzymatic glucosylation. *Environ Microbiol* **21**: 4755–4772.

Whitworth, D.E., and Zwarycz, A. (2020) A genomic survey of signalling in the *Myxococcaceae*. *Microorganisms* **8**: 1739.

Xiao, Y., Wei, X., Ebright, R., and Wall, D. (2011) Antibiotic production by myxobacteria plays a role in predation. *J Bacteriol* **193**: 4626–4633.

© 2021 The Authors. *Environmental Microbiology* published by Society for Applied Microbiology and John Wiley & Sons Ltd.,

Xu, G. (2020) Evolution of LuxR solos in bacterial communication: receptors and signals. *Biotechnol Lett* **42**: 181–186.

Wang, M., Carver, J.J., Phelan, V.V., Sanchez, L.M., Garg, N., Peng, Y., *et al*. (2016) Sharing and community curation of mass spectrometry data with global natural products social molecular networking. *Nat Biotechnol* **34**: 828–837.

Zhang, W., Wang, Y., Lu, H., Liu, Q., Wang, C., Hu, W., and Zhao, K. (2020a) Dynamics of solitary predation by *Myxococcus xanthus* on *Escherichia coli* observed at the single-cell level. *Appl Environ Microbiol*: **86**: e02286-19.

Zhang, Z., Cotter, C.R., Lyu, Z., Shimkets, L.J., and Igoshin, O.A. (2020b) Data-driven models reveal mutant cell behaviors important for Myxobacterial aggregation. *mSystems*: **5**: e00518-20.

Supporting Information

Additional Supporting Information may be found in the online version of this article at the publisher's web-site:

Appendix S1: Supporting Information

Appendix S2: Supporting Information

© 2021 The Authors. *Environmental Microbiology* published by Society for Applied Microbiology and John Wiley & Sons Ltd.,